ANL/MSD/CP-99651

$Pb(Mg_{1/3}Nb_{2/3})O_3$-$PbTiO_3$ Thin Films Synthesized by Metalorganic Chemical Vapor Deposition

S.K. Streiffer[1], G.R. Bai[1], S. Stemmer[2], O. Auciello[1], P.K. Baumann[1], K. Ghosh[1], A. Munkholm[3], C. Thompson[1,4], R.A. Rao[5], and C.-B. Eom[5]

[1]Materials Science Division, Argonne National Laboratory, Argonne, IL 60439-4838
[2]Department of Physics, University of Illinois at Chicago, Chicago, IL 60607-7059
[3]Chemistry Division, Argonne National Laboratory, Argonne, IL 60439
[4]Department of Physics, Northern Illinois University, DeKalb, IL
[5]Department of Mechanical Engineering and Materials Science, Duke University, Durham, NC 27708-0300

Submitted to the US-Japan Seminar on Dielectric and Piezoelectric Ceramics, Okinawa, Japan, held on November 3-5, 1999.

This work was supported by the U.S. Department of Energy, Office of Science Division of Materials Sciences, under contract #W-31-109-ENG-38 and DE-FG02-96ER45610 .

DISCLAIMER

$Pb(Mg_{1/3}Nb_{2/3})O_3$-$PbTiO_3$ Thin Films Synthesized by Metalorganic Chemical Vapor Deposition

S.K. Streiffer*, G. R. Bai*, S. Stemmer§, O. Auciello*, P.K. Baumann*, K. Ghosh*, A. Munkholm†, C. Thompson*‡, R.A. Rao††, and C.-B. Eom††

*Materials Science Division, Argonne National Laboratory, Argonne, IL 60439-4838
fax: 011-630-252-4289, email: streiffer@anl.gov

§Department of Physics, University of Illinois at Chicago, Chicago, IL 60607-7059
fax: 011-312-996-4451, email: stemmer@uic.edu

† Chemistry Division, Argonne National Laboratory, Argonne, IL. 60439
fax: 011-630-252-0365, email: munkholm@anl.gov

‡ Dept. of Physics, Northern Illinois University, DeKalb, IL
fax: 011-630-252-7777, email: c_thompson@anl.gov

††Department of Mechanical Engineering and Materials Science, Duke University, Durham, NC 27708-0300
fax: 011-919-660-5164, email: eom@acpub.duke.edu

Metalorganic chemical vapor deposition was used to synthesize epitaxial $Pb(Mg_{1/3}Nb_{2/3})O_3$-$PbTiO_3$ films on $SrTiO_3$ and $SrRuO_3/SrTiO_3$ substrates, using solid $Mg(DPM)_2$ as the Mg precursor. Deposition conditions have been identified under which phase-pure perovskite PMN-PT may be grown. In contrast, in lead-poor environments, an additional second phases of a disordered magnesium-niobium oxide has tentatively been identified. X-ray diffraction and selected area electron diffraction indicate a cube-on-cube orientation relationship between film and substrate, with a (001) rocking curve width of 0.1°, and in-plane mosaic of 0.8°. The rms surface roughness of a 200nm thick PMN film on $SrTiO_3$ was 2 to 3 nm as measured by scanned probe microscopy. The zero-bias dielectric constant and loss measured at room temperature and 10 kHz for a 350 nm thick pure PMN film on $SrRuO_3/SrTiO_3$ were 1100 and 2%, respectively. Small-signal permittivity ranged from 900 to 1400 depending on deposition conditions and Ti content; low values for the dielectric loss between 1 and 3% were determined for all specimens. Here we report on growth conditions and the initial structural and dielectric characterization of these samples.

1. INTRODUCTION

The relaxor ferroelectric $Pb(Mg_{1/3}Nb_{2/3})O_3$ (PMN) and its solid solution with $PbTiO_3$ (PT) have attracted much attention recently because of excellent dielectric and electromechanical properties [1]. For many applications benefiting from integrated devices, deposition of thin film PMN-PT would be required. It is, however, difficult to synthesize phase pure perovskite PMN films because of the relatively poor stability of the perovskite phase relative to, for example, the pyrochlore phase. Despite this difficulty, a variety of thin film synthesis techniques have been used to fabricate PMN-PT films, including sol-gel [2], sputtering [3], pulsed laser ablation [4], and metalorganic chemical vapor deposition (MOCVD) [5]. Among these methods, and particularly among the vapor-phase techniques, MOCVD offers significant advantages for composition selection and control, film uniformity, high deposition rate, conformality, and scalability to large deposition areas. However, only very limited effort has been directed at obtaining PMN-PT using MOCVD [5]: thin films were grown with perovskite as the main phase only for compositions with Ti/(Mg+Nb+Ti) > 25 mol%, and little information on microstructure was reported. For many applications, it is desirable to obtain not only phase pure but also highly oriented or single-crystal PMN-PT thin films in order to fully utilize the anisotropic piezoelectric properties. Additionally, epitaxial films are essential as model systems so as to better understand properties.

Our goal is to prepare epitaxial $(1\text{-}x)Pb(Mg_{1/3}Nb_{2/3})O_3$-$xPbTiO_3$ thin films with the perovskite structure by MOCVD. Careful control of deposition conditions was used to eliminate impurity phases formed in the preparation of PMN thin films, before PMN-PT films were deposited. Here we report the growth of phase pure, epitaxial PMN and PMN-PT films on (100) $SrTiO_3$ and $SrRuO_3/SrTiO_3$ substrates, using solid $Mg(DPM)_2$ as the Mg precursor. Results from initial structural and electrical characterization are described.

2. FILM GROWTH AND MICROSTRUCTURE

Thin films were grown in a cold-wall, horizontal, low-pressure MOCVD reactor with a resistive substrate heater. Tetraethyl lead, $Pb(C_2H_5)_4$, niobium pentaethoxide, $Nb(OC_2H_5)_5$, solid magnesium β-diketonate, $Mg(C_{11}H_{19}O_2)_2$, and titanium isopropoxide, $Ti(C_3H_7O)_4$, were chosen as the metal ion

precursors. A mixture of the metalorganic precursor vapor was introduced into the reactor via high purity nitrogen carrier gas. The temperatures, pressures, and carrier gas flow rates for each of the precursor chambers were controlled individually, and these parameters were used to adjust the film composition. Pure oxygen was used as the oxidant and introduced into the reactor via a separate delivery line. The precursor delivery lines, as well as the inlet flange, were heated to a temperature higher than the highest source temperature in order to avoid condensation of the vapor phase precursors. Single-side polished, single crystal (001) $SrTiO_3$ was chosen as the substrate for samples used for growth optimization and structural characterization, while (001) $SrRuO_3/SrTiO_3$ substrates were used for PMN-PT samples which were characterized electrically. Immediately prior to deposition, substrates were cleaned with acetone and methanol; no further surface treatments were performed. The typical growth conditions are given in Table I.

Table I: Growth conditions for PMN-PT films

Substrate Temperature:	700°C
Reactor Pressure:	6 Torr
Precursor Temperatures:	Pb: 28 - 30°C Mg: 120 - 140°C Nb: 78 - 84°C Ti: 36°C
Precursor Chamber Pressure:	Pb: 600 Torr Mg: 18 Torr Nb: 18 Torr Ti: 200 Torr
Carrier Gas Flow Rate:	Pb: 20 - 25 SCCM Mg: 36 - 42 SCCM Nb: 55 - 62 SCCM Ti: 18 - 26 SCCM
Oxygen Flow Rate:	400 SCCM
Background N_2 Flow Rate:	100 SCCM
Deposition Rate:	4 - 6 nm/min

The evaporation/sublimation temperatures of the Mg and Nb precursors in our case are somewhat reduced compared to those used by others. Because of this, the MOCVD process reproducibility and controllability were improved significantly.

Film phase content and crystallography were characterized by x-ray diffraction both on a laboratory source and on Beamline 12-ID-D of the Advanced Photon Source. Cu Kα symmetric theta – two theta diffraction spectra are shown in Figures 1 and 2 for a pure PMN film and a PMN-PT film with approximately 20% PT (based on precursor flow rates), respectively, deposited on (001) $SrTiO_3$ substrates. Both films were approximately 300 nm in thickness. Only (00*l*) peaks are observed, with an out-of-plane lattice parameter of 0.406 nm for the PMN sample and 0.402 nm for the PMN-PT sample.

Four circle x-ray diffraction using synchrotron radiation indicated a cube-on-cube orientation relationship between a second 200 nm PMN film and its $SrTiO_3$ substrate, with a (001) rocking curve width of

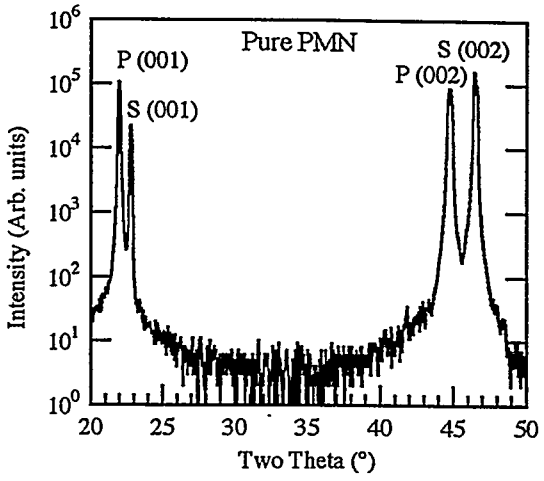

Figure 1: XRD spectrum of a PMN/$SrTiO_3$ sample, showing pure (00*l*) orientation. PMN peaks are indicated by "P", substrate peaks by "S".

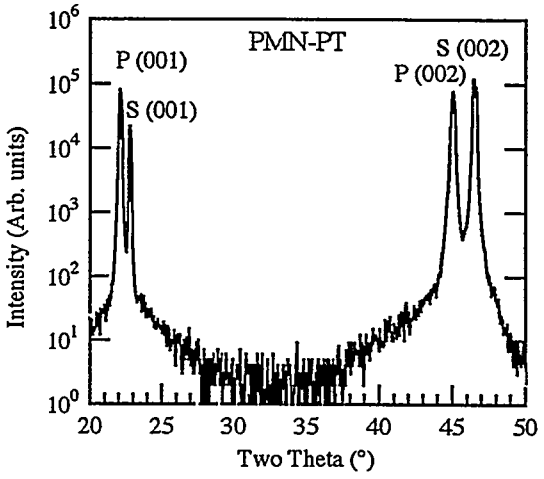

Figure 2: XRD spectrum of a PMN-PT/$SrTiO_3$ sample, showing pure (00*l*) orientation. PMN-PT peaks are indicated by "P", substrate peaks by "S".

0.1° and an in-plane mosaic spread of 0.8°. A tetragonal structure was found for the PMN film, with out-of-plane and in-plane lattice parameters of 0.406 and 0.404 nm, respectively. This tetragonal distortion is most likely the result of the temperature-dependent misfit strain present in the film because of epitaxy with the substrate, and which has only been partially relieved. Additionally, it appears that the unit cell volume of the PMN is slightly expanded relative to the bulk, perhaps because of point defects and/or slight nonstoichiometry in the film. Extremely weak, broad superlattice reflections were found at the (1/2,1/2,1/2) reciprocal lattice positions of the PMN, indicating a very small degree of B-site ordering [6]. The degree of ordering is less than has been observed in, for instance, PMN films prepared by chemical solution deposition [7], and which have experienced higher temperatures of 800 – 850°C.

A scanned probe microscope image of the surface of this sample is shown in Figure 3. The rms roughness of a 2 μm x 2 μm region was 2 nm, with a

maximum peak to valley height of approximately 12 nm. Despite the fact that there is a strong three-dimensional orientation relationship between the PMN and the $SrTiO_3$, the surface microstructure appears granular with a length scale slightly less than 100 nm. This suggests a growth mode with a relatively high nucleation density followed by columnar growth. This is not unexpected given the relatively large lattice mismatch between $SrTiO_3$ and PMN (3.5% at room temperature), and the relatively low growth temperature. These observations are also consistent with the 0.8° in-plane mosaic.

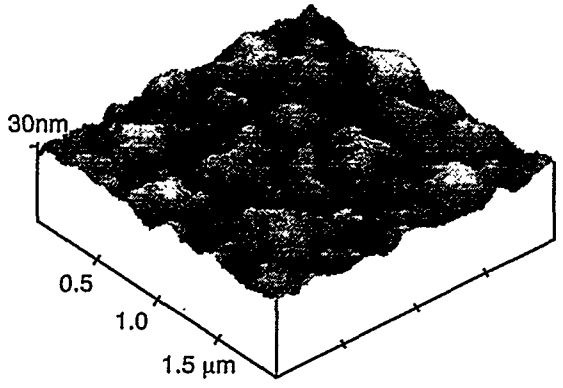

Figure 3: Scanned probe microscope image of the surface of a 200 nm PMN film on $SrTiO_3$. The rms roughness is approximately 2 nm over the 2 μm x 2 μm region.

The samples discussed so far were deposited under optimized conditions, and no impurity phases were detected. In contrast, under non-optimized, lead poor conditions, an impurity peak was found at $2\theta \sim 43.3°$, corresponding to a d-spacing of ~0.21 nm. Furthermore, the impurity peak could be eliminated in the diffraction spectra by increasing the Pb flux and decreasing the Mg flux flowing into the reactor. Depending on the relative amounts of Mg and Nb in the deposited flux, this peak may correspond to $MgNb_2O_6$, (columbite), $Mg_4Nb_2O_9$, which is isostructural with α-Al_2O_3, or possibly to a disordered niobium-magnesium oxide.

To distinguish between these possibilities, cross-sectional transmission electron microscopy was performed, Figure 4. Coherent second phases were observed, as evidenced by stripes of Moiré fringes in the image running in the film thickness direction. The in-plane morphology of the second phase has yet to be determined; it is not clear from the cross-sectional micrographs whether the impurity phase has a planar or perhaps cylindrical microstructure.

Energy dispersive x-ray spectroscopy was performed on the inclusions to determine their composition, yielding a Mg:Nb ratio of 1.4 to 1.9, as compared to 0.5 to 0.6 measured in the film bulk. The out-of-plane lattice parameter and Mg:Nb ratio would appear to be consistent with a (114) or (106) oriented $Mg_4Nb_2O_9$ phase. However, electron diffraction and high-resolution imaging indicate that the impurity phase has a slightly distorted pseudocubic structure, rather than the hexagonal symmetry of bulk $Mg_4Nb_2O_9$.

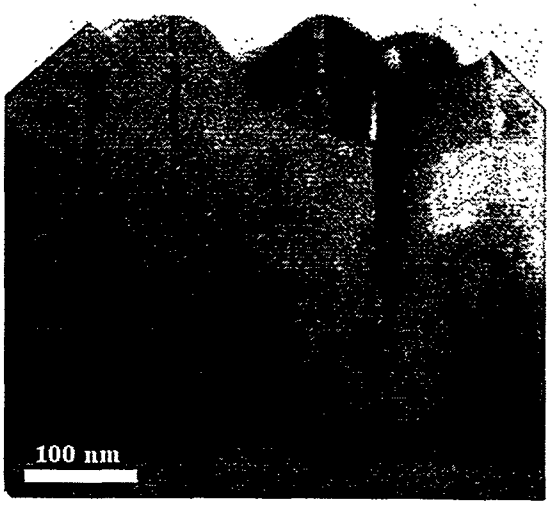

Figure 4: [100] cross-sectional transmission electron microscope image of a PMN film containing the impurity phase

Thus we postulate that the second phase is most likely a disordered magnesium – niobium oxide. More work is need to unambiguously determine the phase's identity. It also should be noted that Figure 4 confirms that these films are comprised of columnar grains separated by low-angle boundaries.

3. DIELECTRIC PROPERTIES

The relative permittivity and dielectric loss as a function of electric field at 10 kHz and 0.2 V oscillation level are given in Figure 5 for a 350 nm pure PMN film on $SrRuO_3/SrTiO_3$, with Pt top electrodes. Hysteresis in the forward and reverse sweeps indicates slim loop, relaxor-like behavior, which is also observed in polarization measurements (not shown).

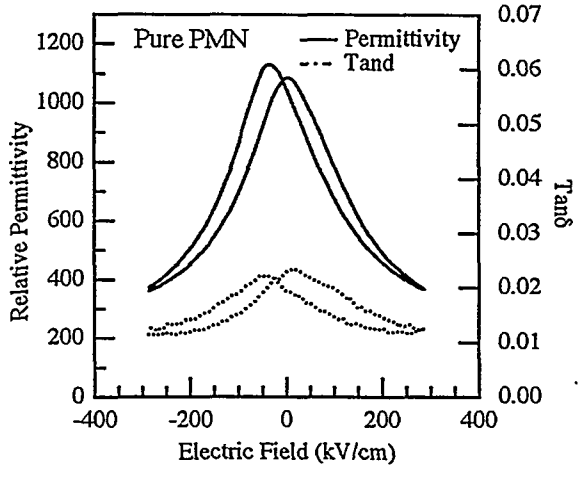

Figure 5: Forward and reverse permittivity – electric field curves taken at 10 kHz for a pure PMN film.

Permittivity as a function of frequency at zero bias is given in Figure 6 for this sample. Dielectric loss is approximately 2% and almost frequency independent over the range that it could be accurately measured, from 1 - 100 kHz, consistent with the modest level of dispersion observed for the permittivity.

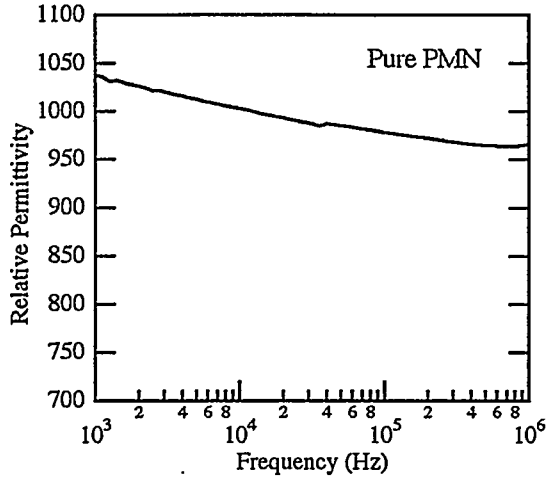

Figure 6: Permittivity vs. frequency at zero bias for a pure PMN film.

Similar results were obtained for PMN-PT films, again with approximately 20% PT. Dielectric constant was found to increase for all samples containing titanium relative to what was measured for pure PMN films, while losses were comparable or slightly higher. Representative forward and reverse permittivity and loss vs. electric field curves are shown in Figure 7. More hysteresis is found for PT-containing samples; however, polarization hysteresis measurements still showed slim loops for these films at room temperature.

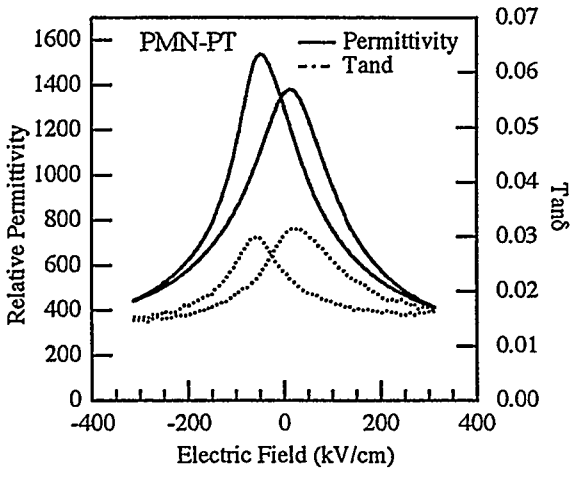

Figure 7: Forward and reverse permittivity – electric field curves taken at 10 kHz for a PMN-PT film.

4. CONCLUSIONS

An MOCVD process was developed for the growth of PMN-PT films, and initial structural and dielectric characterizations have been performed. Although film structural quality is quite high and dielectric losses are low, more work is required to obtain good ferroelectric behavior and square polarization hysteresis loops for these MOCVD samples. Future efforts will center on investigating a wider range of PT contents, and on optimizing the piezoelectric properties of these films.

ACKNOWLEDGMENTS

This work was supported by the U.S. Department of Energy, Basic Energy Sciences – Materials Science through contract #W-31-109-ENG-38 and contract DE-FG02-96ER45610. Use of the APS was supported by the U.S. DOE (BES, OER) also under contract #W-31-109-ENG-38. We thank L. Wills Mirkarimi of Hewlett-Packard for providing some of the $SrRuO_3/SrTiO_3$ substrates used in this work.

REFERENCES

1. Seung-Eek Park and Thomas R. Shrout, *J. Appl. Phys.* **82**, 1804-1811 (1997).
2. K. R. Udayakumar, J. Chen, P.J. Schuele, L.E. Cross, V. Kumar, and S.B. Krupanishi, *Appl. Phys. Lett.* **60**, 1187-1189 (1992). L.E. Francis, and D.A. Payne, *MRS Symp. Proc.* **200**, 173-178 (1990).
3. M.C. Jiang, T.J. Hong, and T.B. Wu, *Jpn. J. Appl. Phys.* **33**, 6301 (1994).
4. K.L Saenger, R.A. Roy, D.B. Beach, and K.F. Etzold, *MRS Symp. Proc.* **285**, 421-426 (1993). Dan Lavric, Rajesh A. Rao, Qing Gan, J.J. Krajewski, and Chang-Beom Eom, *Integrated Ferroelectrics* **21**, 499-509 (1998). J.-P. Maria, W. Hackenberger, and S. Trolier-McKinstry, *J. Appl. Phys.* **84**, 5147-5154 (1998).
5. Yutaka Takeshima, Kosuke Shiratsuyu, Hiroshi Takagi, and Kunisaburo Tomono, *Jpn. J. Appl. Phys.* **34** Pt 1, 5083-5085 (1995).
6. J. Chen, H.M. Chan, and M. Harmer, *J. Am. Cer. Soc.* **72**, 593-598 (1989). Mehmet A. Akbas and Peter K. Davies, *J. Am. Cer. Soc.* **80**, 2933-2936 (1997). Y. Yan, S.J. Pennycook, Z. Xu, and D. Viehland, *Appl. Phys. Lett.* **72**, 3145-3147 (1998).
7. Z. Kighelman, D. Damjanovic, A. Seifert, L. Sagalowicz, and N. Setter, *Appl. Phys. Lett.* **73**, 2281-2283 (1998).